

Accounts

Design and Synthesis of Bis(Zn(II)–Dipicolylamine)-Based Fluorescent Artificial Chemosensors for Phosphorylated Proteins/Peptides

Akio Ojida[1] **and Itaru Hamachi***[1,2]

[1]Department of Synthetic Chemistry and Biological Chemistry, Kyoto University, Kyoto Daigaku Katsura, Kyoto 615-8510

[2]PRESTO (Synthesis and Control, JST)

Received May 16, 2005; E-mail: itarutcm@mbox.nc.kyushu-u.ac.jp

Protein phosphorylation represents a ubiquitous mechanism for controlling diverse protein functions and plays central role in signal transduction cascades in living cells. In order to elucidate the complex network of phosphorylation-based signaling, it is desirable to develop versatile methods and molecular probes that can selectively recognize and detect the phosphoprotein of interest. We present herein the molecular recognition and fluorescence sensing of phosphorylated proteins/peptides by synthetic small molecules. The chemosensors are designed to utilize metal–ligand interaction as a main binding force and thus possess two Zn(II)–dipicolylamine(dpa)s as the binding sites for phosphate group(s) on the protein/peptide surface. We propose the two strategies for recognition of phosphorylated protein/peptide surface; (i) cooperative-binding strategy and (ii) cross-linking strategy. The binuclear anthracene-type chemosensors are designed to interact with a phosphate group on protein/peptide surface based on the cooperative-binding mode, in which the single phosphate group is recognized by the two Zn(II)–dpa sites of the chemosensor. The binding affinity of the chemosensors sensitively depends on the sequence of the phosphopeptide, and reaches to nearly $10^7\,M^{-1}$ for a highly negatively charged peptide. In addition, the chemosensors increase their fluorescence upon binding to the phosphorylated proteins/peptides. Therefore, they can distinguish between phosphorylated and non-phosphorylated state of proteins/peptides by their fluorescence intensities. Detailed experiments clarify that the phosphate anion-assisted binding of the second Zn(II) to the binuclear chemosensors is crucial for the fluorescence increase upon binding to the phosphorylated derivatives. The other approach to recognize phosphorylated protein surface by synthetic small molecule is based on the cross-linking strategy. The chemosensors possess bipyridine as a spacer unit between two Zn(II)–dpa sites, which are arranged at appropriately distal position, thereby make possible the cross-linking interaction with two phosphate groups on protein surface. The chemosensors shows higher affinity for the bis-phosphorylated peptide than for the mono-phosphorylated one, indicating that the cross-linking interaction is effective for recognition of multisite phosphorylation domains of a protein. The results presented in this article are regarded as the first step toward detection of specific phosphorylation event of a protein in complicated biological systems using synthetic small molecules. The bioanalytical application of these chemosensors, such as the fluorescence detection of phosphatase catalyzed dephosphorylation and the selective staining of phosphoprotein in SDS-PAGE, are also discussed.

Post-translational modification by phosphorylation represents a ubiquitous regulatory mechanism for controlling diverse protein functions.[1] Especially, phosphorylation on serine, threonine, or tyrosine residues catalyzed by protein kinase forms the basis of cell signaling networks, in which protein functions are controlled by reversible phosphorylation with spatio-temporal fashions in response to changes of the cellular environment. For example, phosphorylation acts as a molecular switch to turn on protein activity.[2] A typical example of such allosterical function control is observed in MAPK (mitogen-activated protein kinase), in which the activation loop of the kinase undergoes a conformational change upon phosphorylation of the threonine and tyrosine residues within the loop, resulting in recovery of the kinase activity due to unrestricted access of ATP and protein substrates to the kinase active site.[3] Protein phosphorylation also has an important role in controlling the reversible assembly of a signaling complex.[4,5] Attachment of a phosphate group creates new interaction sites on protein surfaces, which are recognized by downstream proteins that contain phosphoprotein-binding domains to form a multiprotein complex. Various types of conserved phosphoprotein-binding domain such as SH2, PTB, FHA, and WW domain are found in many signaling proteins. It is also known that protein phosphorylation acts as a dynamic mechanism for controlling the subcellular localization and activity of many transcription factors.[6]

Published on the web January 13, 2006; DOI 10.1246/bcsj.79.35

In order to decipher the complex network of phosphorylation-based cell signaling, it is highly desirable to develop versatile methods and molecular probes that can selectively recognize and detect a phosphoprotein of interest. A phosphospecific antibody is a useful tool for the detection of phosphorylation state of a protein, and has already been exploited for many different applications, including immunohistochemistry and flow cytometry, to monitor kinase activity in cells.[7] However, use of the antibody is sometimes restricted by its large size, which may cause interference of the function or structure of the target phosphoprotein. Recently, a number of molecular devices that can fluorometrically sense specific protein kinase activity have been developed.[8] They consist of a substrate sequence that is directly connected to a sensoring unit, in which the phosphorylation of substrate units by a specific kinase is detected by the fluorescent signaling change. For example, various kinds of FRET-based biosensor using CFP and YFP as a donor–acceptor system have been developed for visualizing the kinase activity in living cell.[9] Phosphorylation-responsive fluorescently tagged peptides have also been extensively developed for in vitro and in vivo kinase activity assay.[10] We are interested in the development of small molecules that can directly interact with phosphate group(s) on a protein surface.[11] We anticipate that such molecular probes will enable us to detect the dynamic change of the phosphorylation/dephosphorylation state of protein of interest, and thus offer a means of investigating phosphorylation-based cell signaling. Furthermore, it is expected that these probes will not only be useful as analytical tools for protein phosphorylation event but will also serve as artificial regulators for functions of specific phosphoprotein.

In this review, we describe the binding and sensing properties of a new class of artificial chemosensors for phosphorylated proteins/peptides, which recognize and fluorometrically sense phosphate group(s) of protein/peptide surfaces using metal–ligand interaction. These chemosensors are designed based on the two strategies for phosphorylated protein/peptide recognition; one is for recognition of single phosphate group by cooperative action of two Zn(II)–dpa sites (i.e., the cooperative-binding strategy, Fig. 1a), and the other is for simultaneous recognition of two phosphate groups on protein/peptide surface by two Zn(II)–dpa sites via a chelation-like manner (i.e., the cross-linking strategy, Fig. 1b). We also present some biological applications of these chemosensors, which successfully demonstrate their utilities in biological analysis.

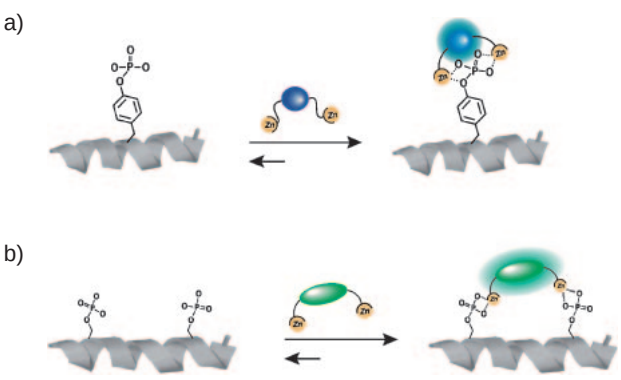

Fig. 1. Two strategies for phosphorylated protein/peptide recognition by chemosensors.

Artificial Chemosensors for Single Phosphate Groups on Protein Surfaces[12,13]

Molecular Design

Phosphate group attached on a protein surface by kinase-catalyzed reaction interacts with many amino acid residues inter- and intra-molecularly, in which multiple hydrogen-bonding and ion-pair interactions are formed in spatially arranged manners. In these cases, a phosphate group plays a central role to construct a defined protein structure and/or a signaling protein complex by accumulating these weak interactions. In contrast to the sophisticated recognition system of a phosphate group on protein surface in nature, the artificial receptors and chemosensors for phosphate anions are still in their early stages. To date, a number of artificial receptors and chemosensors for phosphate anion have been reported, most of which utilize hydrogen-bonding and electrostatic interactions as the main binding forces.[14,15] However, they are not able to form tight any binding complex with phosphate species in aqueous medium because of the ineffectiveness of combining usage of these interactions in a water system in general. In a pioneering work by Czarnik et al., the polyamine-appended anthracene was reported as a fluorescent sensor for phosphate anion, in which multiple hydrogen-bonding and ion-pair interactions between the amino groups and phosphate anion were employed as the main binding forces.[16] However, the binding affinity is not high enough to apply this chemosensor to biological systems involving phosphorylated proteins/peptides. We planned to utilize a metal–ligand interaction (i.e., coordination chemistry) as a main force to bind phosphate species, since this interaction should work more effectively in water compared to the other weak interactions.[17–19] In nature, there are many examples of metalloenzymes possessing two or more metal centers in their active sites.[20] For example, alkaline phosphatase, a hydrolysis enzyme for phosphomonoester, possesses two zinc ions in its catalytic active site, which are oriented in the close proximity suitable for the bidentate binding with a phosphate anion. By mimicking such a natural anion recognition system, we designed chemosensor **1** and **2** bearing the two sets of Zn(II)–dpa (dipicolylamine)s in an appropriate distance (Fig. 2). We also expected that the phosphate binding event might be read out by changing of photochemical behavior of a fluorophore positioned close to the phosphate binding site. Thus, we selected an anthracene as a typical fluorophore, which are connected to the two Zn(II)–dpa sites in **1** and **2** through a C1 methylene unit.

Selective Fluorescence Sensing for Phosphate Anion. Figure 3a shows the fluorescent sensing behavior of chemosensor **1** toward *o*-phospho-L-tyrosine (p-Tyr). The fluorescence increased in intensity due to the anthracene moiety and showed a typical saturation behavior depending on the p-Tyr concentration. The fluorescence enhancement was also observed in the titrations with other phosphorylated species such as hydrogenphosphate anion (HPO_4^{2-}), and phosphate monoesters (phenyl phosphate (PhP), *o*-phospho-L-tyrosine (p-Tyr), and methyl phosphate (MeP)). Table 1 summarizes the apparent binding constants (K_{app}, M^{-1}) of **1** and **2** for these phosphate species estimated by the fluorescence titration. Clearly, these chemosensors showed a high affinity toward the monophosphate derivatives with 10^5–10^4 M^{-1} of the binding con-

stants in aqueous solution. It was also observed that the chemosensors exhibit the stronger binding affinity toward the diphosphate derivatives such as ATP and ADP compared to the monophosphate species. Interestingly, dimethyl phosphate (diMeP) and cyclic AMP (cAMP) did not cause any fluorescence change up to millimolar concentration range, suggesting that **1** and **2** can distinguish phosphate and phosphate monoesters from phosphate diesters. On the other hand, the chemosensors did not change their fluorescence intensities upon addition of other anions in the micromolar concentration range (Fig. 3b). Although addition of hydrogen carbonate gradually intensified the fluorescence in the 10^{-3} M range of concentration, no fluorescence response was induced by other anions such as sulfate, nitrate, acetate, chloride, and fluoride. These results reveal that **1** and **2** are fluorescent chemosensors with a high selectivity toward phosphate species among the various anions. In contrast, the mononuclear chemosensor **3** did not show any fluorescence changes for these phosphate derivatives under the same conditions. The affinity of the mononuclear Zn(II)–dpa complex toward phosphate derivatives was evaluated by a fluorescence competitive inhibition experiment.[21] The binding between **2** and phenyl phosphate was inhibited depending on the amount of **5** added (50–300 equiv), and

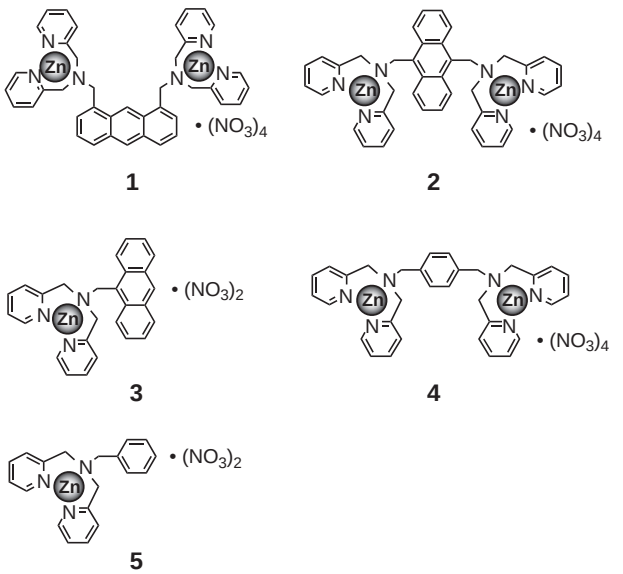

Fig. 2. Molecular structure of the chemosensors and the derivatives.

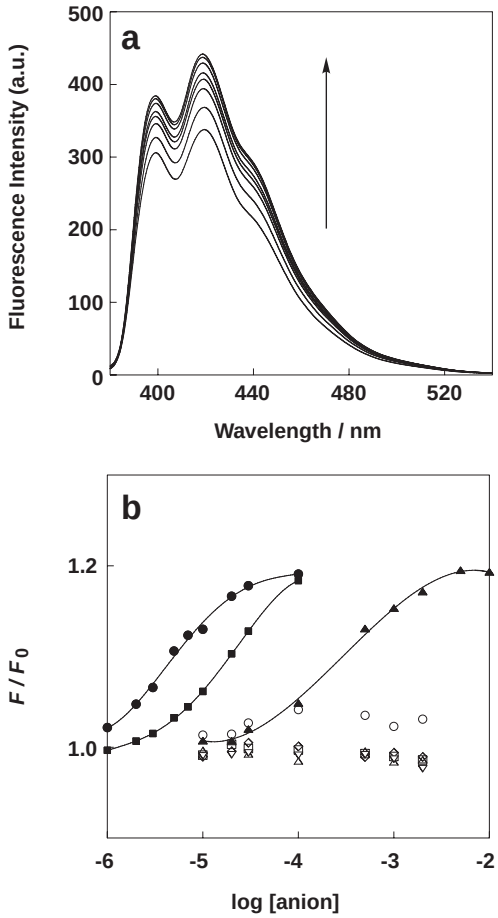

Fig. 3. (a) Fluorescence spectral change of **1** (5 μM) upon addition of *o*-phospho-L-tyrosine (p-Tyr): [p-Tyr] = 2.5, 5, 7.5, 10, 15, 20, and 25 μM. (b) Relative fluorescence emission response of **1** to the anion concentration: phosphate (●), p-Tyr (■), sulfate (□), nitrate (◇), acetate (○), carbonate (▲), chloride (△), and fluoride (▽). Measurement conditions: 10 mM HEPES, pH 7.2, 20 °C, and λ_{ex} = 370 nm.

Table 1. Summary of the Apparent Binding Constant (K_{app}, M^{-1}) of **1** and **2** to the Phosphate Species by Fluorescence Change

Phosphate species[a)]	Chemosensor		Phosphate species[a)]	Chemosensor	
	1	**2**		**1**	**2**
NaH_2PO_4[b)]	4.2×10^5	2.9×10^5	ATP[c)]	$>10^7$	4.0×10^5
PhP[b)]	2.1×10^5	5.1×10^4	ADP[c)]	$>10^7$	1.6×10^5
p-Tyr[b)]	3.1×10^5	6.1×10^5	AMP[c)]	2.3×10^5	9.1×10^3
MeP[b)]	1.1×10^5	7.9×10^3	cAMP[c)]	—[d)]	—[d)]
diMeP[b)]	—[d)]	—[d)]			

a) PhP = phenyl phosphate, p-Tyr = *o*-phospho-L-tyrosine, MeP = methyl phosphate, diMeP = dimethyl phosphate, ATP = adenosine 5′-triphosphate, ADP = adenosine 5′-diphosphate, AMP = adenosine 5′-monophosphate, cAMP = adenosine 3′,5′-cyclic monophosphate. Measurement conditions: b) 10 mM HEPES, pH 7.2, and 20 °C. c) 50 mM HEPES, 50 mM NaCl, pH 7.2, and 20 °C. d) Since the fluorescence change was scarcely observed, the association constant cannot be obtained.

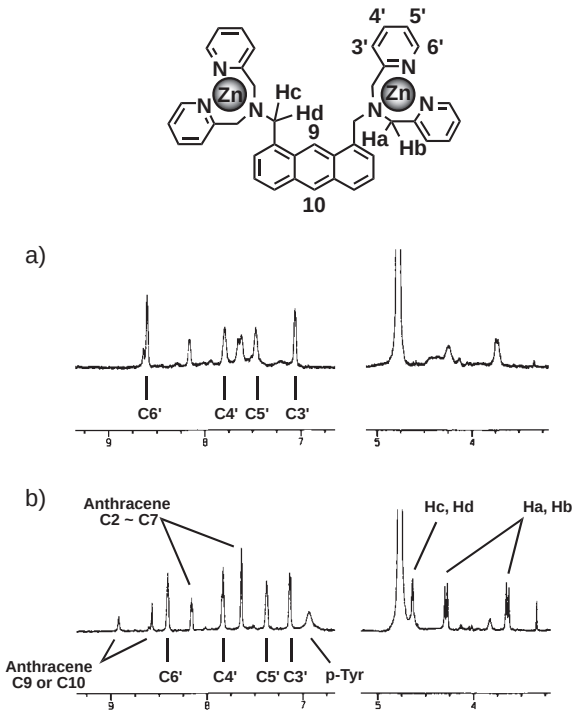

Fig. 4. ^{1}H NMR spectra of **1** (0.1 mM) in the absence (a) and in the presence (b) of 1 equiv of p-Tyr measured in D_2O, pD 7.1 ± 0.1.

the analysis of the obtained data afforded the apparent binding constant (*Ki*) of **5** for phenyl phosphate as 3–4 × 10^3 M^{-1}, which is one or two orders of magnitude lower than those of **1** or **2**. This result suggests that the two Zn(II)–dpa sites are indispensable for the tight binding and sensing of phosphate derivatives in aqueous solution.

Binding Mode of the Zn(dpa)-Based Chemosensors to Phosphate Species. A ^{1}H NMR study gave insight into the complex structure of **1** with p-Tyr in aqueous solution. Figure 4 shows the ^{1}H NMR signals of the aromatic and methylene regions of **1** in D_2O (pD 7.1 ± 0.1). Upon addition of 1 equiv of p-Tyr, the proton signals of the pyridine rings slightly upfield-shifted (0.09–0.18 ppm) and were not distinguishable among the four pyridine rings of the two sets of dpas. Furthermore, the signals of two sets of three methylene protons connected to the tertiary nitrogen (4.63, 4.29, and 3.65 ppm) became sharper upon the p-Tyr binding. These observations suggest that the two Zn(II)–dpa sites of **1** equally contribute to the binding to p-Tyr. In the ^{31}P NMR study, the chemical shift due to the phosphorus of p-Tyr moved from −2.09 to −3.00 ppm upon addition of 1 equiv of **1**. The similar upfield shift of the ^{31}P NMR signal was observed in the case of phenyl phosphate (from −2.72 to −3.94 ppm), and a phosphorylated peptide KSGpYLSSE (from −2.12 to −2.90 ppm). These results suggest that chemosensor **1** directly interacts with their phosphate sites in aqueous solution.

We unequivocally determined the binding structure of chemosensor **1** with a phosphate species by X-ray crystallographic analysis of a complex with phenyl phosphate (PhP). As shown in Fig. 5a, **1** and PhP form a 2:2 complex related by a symmetric center in the unit cell. In the asymmetric half unit (Fig. 5b), it is clear that **1** binds PhP by using the two sets

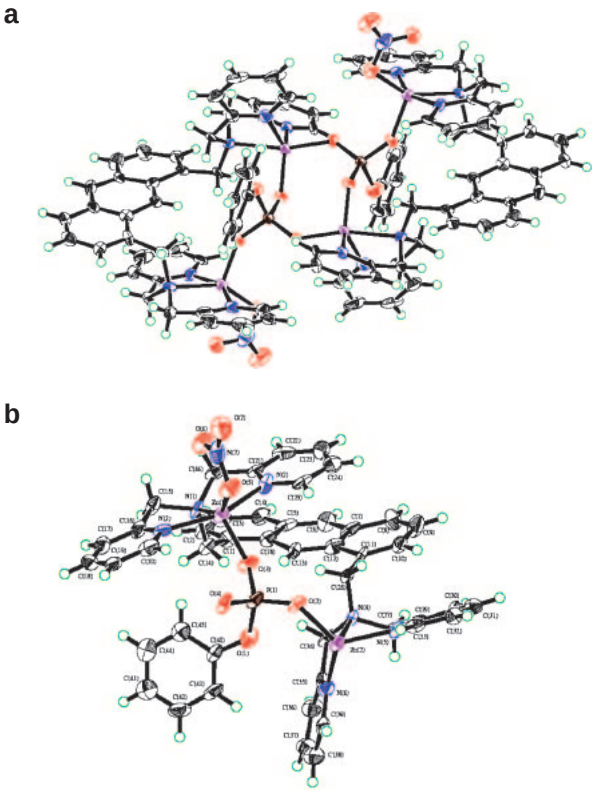

Fig. 5. ORTEP drawing (50% probability ellipsoids) of the complex of **1** with phenyl phosphate: (a) a dimer complex and (b) an asymmetrical half unit of the complex. Disordered nitrate anions are omitted for clarity.

of Zn(II)–dpas through the coordination interactions between the Zn(II) ions and the phosphate group. This cooperative action of the two Zn(II)–dpa sites is quite consistent with the other experimental data obtained in aqueous solution and reasonably explains the high affinity of **1** toward phosphate species compared to the monodentate derivatives **3** and **5**.

On the other hand, structural information of the binding complex with phosphate species was not obtained in the case of **2**, neither by NMR or X-ray crystallographic analysis. This is partially due to the aggregation property of **2** under relatively high concentration conditions (>0.1 mM). However, the observed strong binding affinity of **2** for phosphate species (Table 1) indicates the cooperative use of the both Zn(II)–dpa sites for phosphate binding, as clearly exemplified in **1**.

Binding and Fluorescence Sensing toward Phosphorylated Peptide. Subsequently, we explored the fluorescent sensing ability of the chemosensors for phosphorylated peptides. Figure 6 shows a typical fluorescence spectral change of **1** during the titration with a phosphorylated peptide. The fluorescence intensity of the chemosensor significantly increased ($F/F_0 = 2.5$) by the addition of less than 2 μM of peptide-a (EEEIpYEEFD), a consensus sequence phosphorylated by a protein kinase, v-Src. In sharp contrast, little fluorescence change took place due to the corresponding non-phosphorylated peptide-g, showing that the chemosensor can perfectly distinguish the phosphorylated peptides from a non-phosphorylated one. The sequence selective recognition and the sensing ability of the chemosensors were also examined using a

series of phosphorylated peptides. These peptides possess a distinct number of net charges from −8 to +2 (from peptide-a to peptide-f) and contain the optimal consensus sequences of various protein kinases[22,23] with the exception of peptide-d which is the fragment of ezrin (142–149) phosphorylated by EGFR kinase.[24] The results of the fluorescent titration experiments of **1** and **2** with these peptides are summarized in Fig. 7 and Table 2. Interestingly, the binding constant of the chemosensors becomes greater with increase in the negative charge of the phosphorylated peptides. Both chemosensors show the strongest binding affinity with peptide-a having the largest negative charge (−8) with K_{app} of 10^7–10^6 M^{-1}. In the case of peptides-e and -f bearing the net charges of 0 and +2, respectively, the chemosensors can scarcely sense them even for 10^{-4} M of concentration. A typical photograph of the fluorescence change of the chemosensor **2** upon addition of peptide-a is displayed in Fig. 8. It is apparent that the blue fluorescence of **2** is greatly intensified by the phosphorylated peptide-a, whereas the non-phosphorylated peptide-g does not induce any fluorescence change.

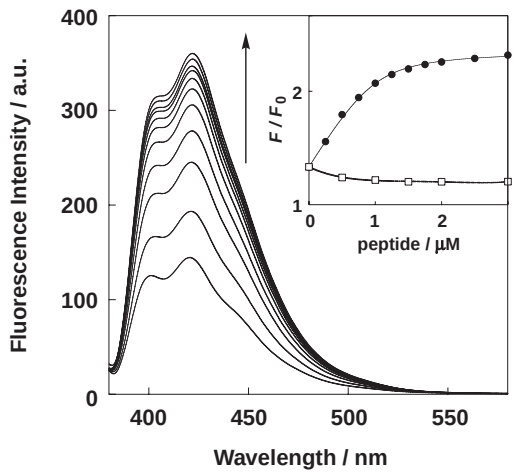

Fig. 6. Fluorescence spectrum change of **1** (1 μM) upon addition of peptide-a: [peptide-a] = 0, 0.25, 0.5, 0.75, 1, 1.25, 1.5, 1.75, 2, 2.5, and 3 μM in 50 mM HEPES, 50 mM NaCl, pH 7.2, 20 °C, and λ_{ex} = 370 nm. (Inset) Fluorescence titration curve of **1** with peptide-a (●) and peptide-g (□). The titration data of peptide-a was analyzed by the nonlinear least-square curve-fitting method assuming 1:1 binding.

The binding of the chemosensors with the series of the phosphorylated peptides was also evaluated by isothermal titration calorimetry (ITC).[25] Figure 9 shows typical titration data of **1** with the peptide-d, and the obtained thermodynamic parameters are shown in Table 3. The resultant binding isotherm is well fitted with a curve derived from 1:1 binding algorithm (n = 1.05) to yield a binding constant of $4.39 \pm 0.55 \times 10^5$ M^{-1}. Interestingly, the interaction is an entropy-driven endo-

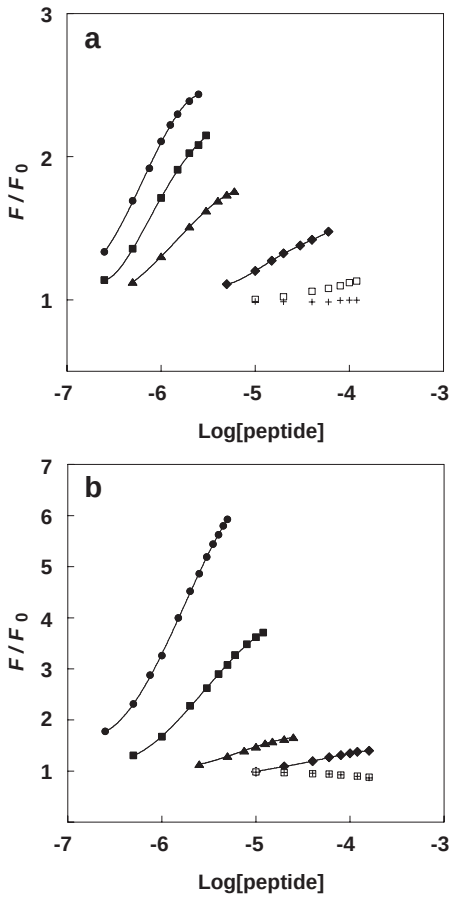

Fig. 7. Fluorescence titration profiles of **1** (a) and **2** (b) with phosphorylated peptides a–f: peptide-a (●), peptide-b (■), peptide-c (▲), peptide-d (◆), peptide-e (□), and peptide-f (+). Measurement conditions: (a) 50 mM HEPES, 50 mM NaCl, pH 7.2, 20 °C, and λ_{ex} = 370 nm, (b) 50 mM HEPES, 10 mM NaCl, pH 7.2, 20 °C, and λ_{ex} = 380 nm.

Table 2. Amino Acid Sequences of the Peptides Containing Optimal Consensus Sequences Phosphorylated by Different Protein Kinases and Apparent Binding Constant (K_{app}, M^{-1}) of **1** and **2** to the Peptides Determined by Fluorescence Change

	Consensus Substrate Sequence	Kinase	Net Charge	**1**	**2**
peptide-a:	Glu-Glu-Glu-Ile-pTyr-Glu-Glu-Phe-Asp	*v*-Src	−8	8.9×10^6	9.5×10^5
peptide-b:	Asp-Glu-Glu-Ile-pTyr-Gly-Glu-Phe-Phe	*c*-Src	−6	1.5×10^6	3.6×10^5
peptide-c:	Ala-Glu-Glu-Ile-pTyr-Gly-Val-Leu-Phe	Lck1	−4	8.2×10^5	1.5×10^5
peptide-d[a]:	Lys-Ser-Gly-pTyr-Leu-Ser-Ser-Glu	EGFR	−2	5.8×10^4	1.2×10^4
peptide-e:	Ala-Arg-Arg-Gly-pSer-Ile-Ala-Ala-Phe	PKA	0	—[b]	—[b]
peptide-f:	Arg-Arg-Phe-Gly-pSer-Ile-Arg-Arg-Phe	Bck1	+2	—[b]	—[b]
peptide-g:	Glu-Glu-Glu-Ile-Tyr-Glu-Glu-Phe-Asp	*v*-Src		—[b]	—[b]

a) Amino acid sequence of ezrin (142–149) phosphorylated by EGFR. b) Since the fluorescence change was scarcely observed, the association constant cannot be obtained.

thermic process ($\Delta S > 0$, $\Delta H > 0$), presumably due to the release of water molecules from the solvent sphere around the chemosensor and/or the phosphopeptide.[26] Due to the aggregation property of chemosensor **2** under the high concentration necessary for ITC measurement (25–100 μM), the compound **4** was used as a structurally related analogue of **2**. As shown in Table 3, all of the interactions are endothermic processes ($\Delta H > 0$), and the binding stoichiometry (values n) is estimated to be approximately 1. It is to be noted that the evaluated binding constants for peptide-c and peptide-d are in good agreement with those obtained by the fluorescence titration under the same conditions (Table 3). The binding constants of **1** to peptide-e and peptide-f, which cannot be fluorometrically detected, were determined to be $1.12 \pm 0.12 \times 10^4$ and $5.28 \pm 2.27 \times 10^3\ M^{-1}$, respectively, by ITC experiment. These values are more than 100-fold smaller than those for peptide-a and peptide-b.

Both the fluorescence and ITC experiments undoubtedly demonstrate that the chemosensors can discriminate the sequence of the phosphorylated peptide and more strongly bind to the negatively charged one. Since the present binuclear chemosensors possess a tetracationic character, it is reasonable to propose that the electrostatic attraction can assist the coordination interaction between the chemosensors and the negatively charged peptides such as peptide-a, whereas the electrostatic repulsion significantly suppresses the affinity toward the positively charged peptides such as peptide-e and peptide-f. The resulting order of the binding constants for these peptides in our experiments is consistent with this explanation. It is noteworthy that even the structurally simple chemosensors of ours show such a sequence-dependent recognition toward the phosphorylated peptides.

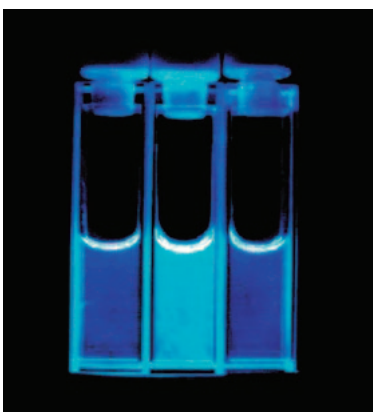

Fig. 8. Photograph of the increased emission of **2** in the presence of phosphorylated peptide-a (middle) compared to **2** only (left) and **2** with non-phosphorylated peptide-g (right).

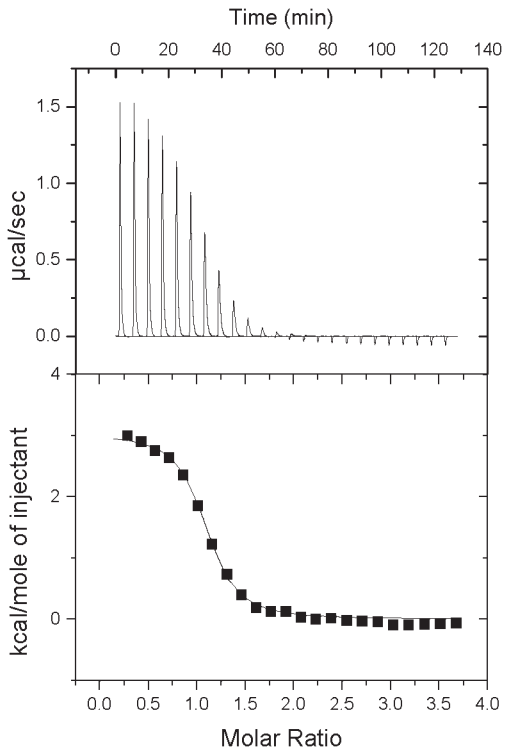

Fig. 9. A typical ITC titration curve and processed data for the titration of **1** with peptide-d. Measurement conditions: [**1**] = 100 μM, [peptide-d] = 2.0 mM (24 × 10 μL injections), 50 mM HEPES, pH 7.2, and 25 °C.

Table 3. Stoichiometry (n), Binding Constant (K_{app}, M^{-1}), Enthalpy (ΔH, kcal mol^{-1}), and Entropy ($T\Delta S$, kcal mol^{-1}) for Interaction of Chemosensor **1** and **4** with the Phosphorylated Peptides

Chemosensor		peptide-a	peptide-b	peptide-c	peptide-d	peptide-e	peptide-f
1	n			0.88 ± 0.01	1.05 ± 0.01	0.93 ± 0.07	1.26 ± 0.48
	K_{app}	$>10^7$	—[b]	$(1.81 \pm 0.38) \times 10^6$ (1.3×10^6)[c]	$(4.39 \pm 0.55) \times 10^5$ (3.5×10^5)[c]	$(1.12 \pm 0.12) \times 10^4$	$(5.28 \pm 2.27) \times 10^3$
	ΔH			3.79 ± 0.08	3.01 ± 0.04	3.23 ± 0.32	0.79 ± 0.40
	$T\Delta S$			12.32	10.70	8.75	5.86
4	n			0.98 ± 0.01	0.98 ± 0.02		
	K_{app}	—[a]	—[b]	$(8.34 \pm 0.11) \times 10^5$ (7.9×10^5)[d]	$(4.99 \pm 0.34) \times 10^4$ (2.9×10^4)[d]	$<10^3$	$<10^3$
	ΔH			4.49 ± 0.07	3.26 ± 0.07		
	$T\Delta S$			12.56	9.66		

a) Accurate value cannot be obtained under the ITC measurement conditions. b) Due to the insolubility of the peptide, the data cannot be obtained. c) Apparent binding constant of **1** obtained by the fluorescence titration under the same conditions (50 mM HEPES and pH 7.2). d) Apparent binding constant of **2** obtained by the fluorescence titration under the same conditions (50 mM HEPES buffer and pH 7.2).

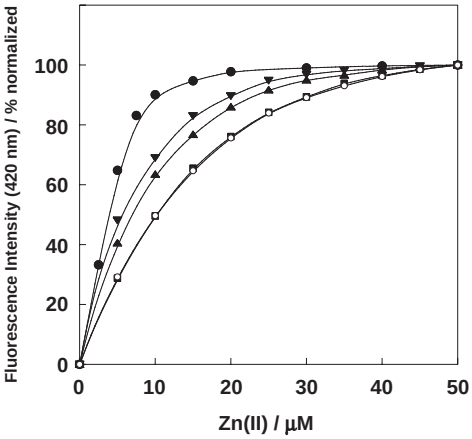

Fig. 10. Fluorescence response of the Zn(II)–free ligand of **1** (5 μM, $\lambda_{ex} = 370$ nm) to Zn(II) concentration in 50 mM HEPES and pH 7.2: **1** (■), **1** in the presence of 1 equiv of p-Tyr (▲), 4 equiv of p-Tyr (▼), 2 equiv of peptide-a (●), and 10 equiv of dimethyl phosphate (○).

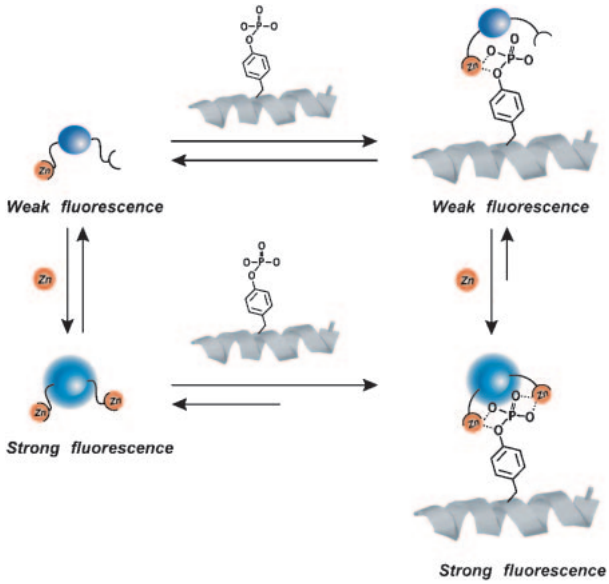

Fig. 11. Schematic representation of the sensing mechanism of the chemosensors toward the phosphorylated peptide.

Mechanism for Fluorescence Sensing of Phosphorylated Peptide. The fluorescence enhancement of the chemosensors by binding to the phosphorylated peptides is ascribed to the canceling of photoinduced electron-transfer (PET) process induced by the phosphate anion-assisted Zn(II) binding. Figure 10 shows the Zn(II) concentration dependence of the fluorescence intensity of the Zn(II)–free ligand of **1**. Under neutral pH conditions, the fluorescence of **1** and **2** due to the anthracene moiety was intensified by the addition of Zn(II). This fluorescence enhancement is reasonably explained by Zn(II) binding to the benzylic amine of the dpa site by canceling of the photoinduced electron-transfer (PET) process, a typical sensing mechanism of fluorogenic chemosensors for d^{10} metal such as Zn(II).[27] Interestingly, more than 5 equiv of Zn(II) is required for saturation of the fluorescence enhancement. From the fluorescence titration experiments, the apparent complexation constant of the first and second Zn(II) with the free ligand **1** was evaluated to be $>1 \times 10^6$ and $\sim 3 \times 10^5\ M^{-1}$, respectively, suggesting that the second Zn(II) does not fully complex with the dpa site under the low micromolar concentration ($\sim$5 μM). The lower affinity of the second Zn(II) to dpa is probably due to the electrostatic repulsion between the positively charged first Zn(dpa) site and the incoming second Zn(II) cation. The second Zn(II) complexation constant of **2** was also evaluated to be $\sim 7 \times 10^4\ M^{-1}$, indicative of the partial interaction of the second Zn(II) to the dpa site under low micromolar concentration. Importantly, when Zn(II) was added to the free ligand of **1** or **2** in the presence of p-Tyr, the fluorescence change was more sharply saturated depending on the amount of p-Tyr (1 or 4 equiv) relative to that in the absence of p-Tyr (Fig. 10). This indicates that binding of the second Zn(II) to the free dpa site is facilitated by p-Tyr. The same magnitude of enhancement was also observed with NaH_2PO_4 and MeP, and, interestingly, the fluorescence change was saturated with almost 2 equiv of Zn(II) in the presence of peptide-a, which can strongly bind to **1** ($K_{app} = 8.9 \times 10^6\ M^{-1}$). In contrast, the excess amount of diMeP (10 equiv), which cannot bind to chemosensor **1**, does not cause any facilitation effect on the Zn(II) binding. Almost the same tendency was observed for chemosensor **2** with these phosphate species. These results strongly suggest that the phosphate-assisted binding of the second Zn(II) is responsible for the fluorescence intensification of chemosensors **1** and **2**. A schematic illustration of the sensing mechanism toward the phosphorylated peptide is depicted in Fig. 11. In the absence of a phosphorylated peptide, the second dpa site of the chemosensor is partially free so that the PET quenching by the benzylic amine of dpa lessens the fluorescence of the anthracene. In the presence of a phosphorylated peptide, binding of the second Zn(II) to the free dpa site is facilitated, and as a result, the PET quenching is suppressed and the fluorescence intensity recovers. Recently, Lawrence et al.[28] and Imperiali et al.[29] have reported some peptide-based fluorescent probes for protein kinase activity that possess the sensing mechanism analogous to that of our chemosensors. In these sensing systems, a phosphate group attached to the substrate peptide by a kinase reaction intra-molecularly induces Ca^{2+} or Mg^{2+} binding to the fluorophore that is adjacently connected to the phosphorylation residues, which consequently results in the fluorescence enhancement. By contrast, our chemosensors efficiently utilize this sensing mechanism in an intermolecular manner based on the molecular recognition.

Biological Application of the Chemosensors. On the basis of the binding and fluorescence sensing properties of the chemosensors toward phosphorylated peptides, we successfully demonstrated the utility of the chemosensors in two biological assay, that is, the fluorescent monitoring of phosphatase-catalyzed dephosphorylation and the selective staining of phosphoprotein in SDS-PAGE.

The fluorescence sensing ability of the chemosensor toward phosphopeptide was successfully applied to monitoring an enzymatic dephosphorylation process catalyzed by phosphatase PTP1B. As shown in Fig. 12, the fluorescence intensity of **1** enhanced by binding to the substrate phosphopeptide DADE-pY-LIPNNG (a fragment (988–998) of EGFR) decreased time-

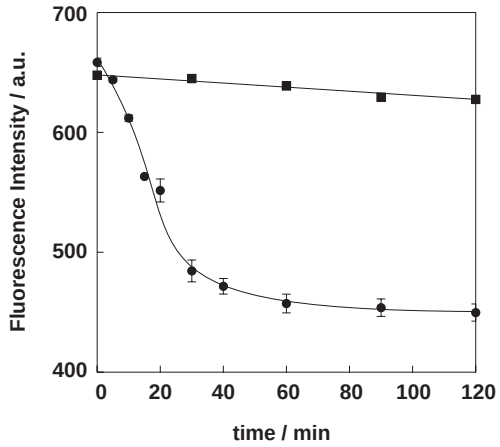

Fig. 12. Time trace of the PTP1B-catalyzed dephosphorylation monitored by the emission (at 420 nm) of **1** ($\lambda_{ex} = 370$ nm) with (●) or without (■) PTP1B using the fluorescence plate reader.

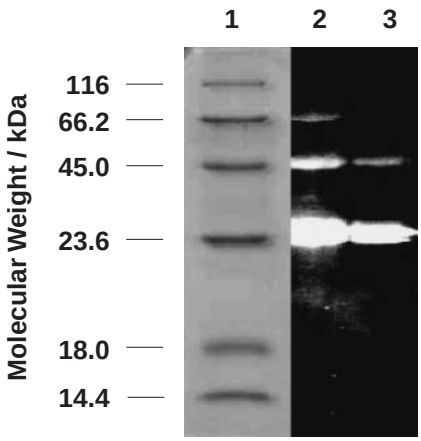

Fig. 13. Selective phosphoprotein detection in SDS-polyacrylamide gels using **2**. Each lane includes two phosphorylated proteins (ovalbumin (45.0 kDa) and α-casein (24.0 kDa)), and four non-phosphorylated proteins (β-galactosidase (116 kDa), bovine serum albumin (66.2 kDa), avidin (18.0 kDa), and lysozyme (14.4 kDa)). Lane 1; CBB staining of the six proteins. Lane 2, 3; Detection of the phosphoproteins with UV transilluminator after staining with **2**. The amount of each protein in lane 2 and lane 3 is 5.0 and 2.5 μg, respectively.

dependently after the addition of PTP1B according to approximately first-order kinetics. This is ascribed to the fact that the affinity of the chemosensor toward the anionic substrate peptide is stronger than that for the produced phosphate anion. The dephosphorylation process was also successfully monitored by chemosensor **2** in a similar manner. We expect that this assay system can be readily extended to a screening assay for certain kinds of phosphatase inhibitors, including the PTP1B inhibitor that has been a promising therapeutic agent for type II diabetes and obesity.[30]

The utility of the chemosensors as a chemical probe was also demonstrated in selective staining of phosphoprotein in SDS-PAGE (sodium dodecyl sulfate-polyacrylamide gel electrophoresis).[31] We employed **2** as a fluorescent staining reagent

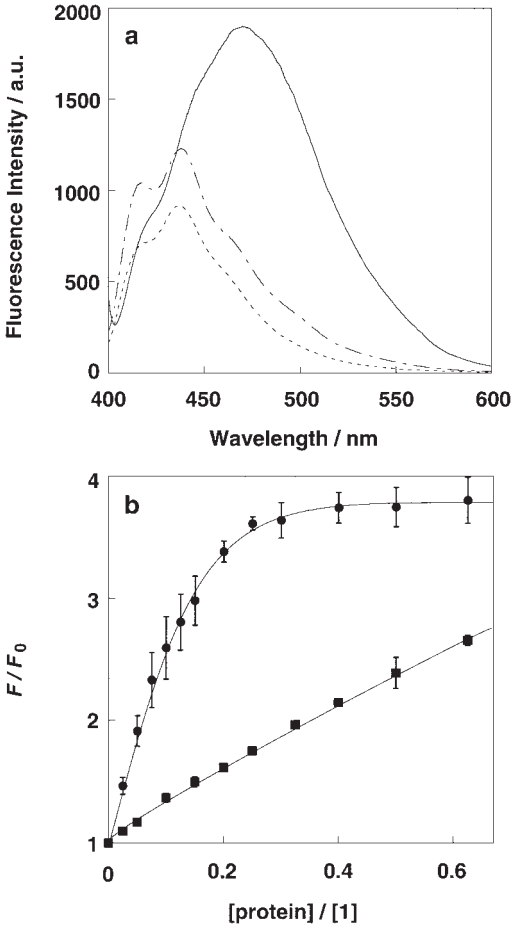

Fig. 14. (a) Fluorescence intensity of **2** (1 μM) in the absence (broken line) and in the presence of 0.25 μM phospho-α-casein (solid line) or dephospho-α-casein (dot-dash line) in 50 mM HEPES, pH 7.2, 20 °C, and $\lambda_{ex} = 380$ nm. (b) The titration curves of the integrated fluorescent change of **2** with phospho-α-casein (●) or dephospho-α-casein (■).

after the conventional gel electrophoresis of the protein mixtures. As shown in Fig. 13, only two distinct bands were fluorescently observed under the photo-illumination using a UV transilluminator; the band correspond to phospho-ovalbumin (MW = 45.0 kDa) and phospho-α-casein (MW = 23.6 kDa). Although a weak emission was observed as the band corresponding to hydrophilic BSA (bovine serum albumin) probably due to a nonspecific absorption (Lane 2, 5.0 μg of each protein), the non-phosphorylated four proteins were not detected in Lane 3 (2.5 μg of each protein). Figure 14a shows the fluorescence spectral changes of **2** induced by highly phosphorylated phospho-α-casein (8–9P) and dephospho-α-casein (1–2P) under the aqueous conditions (50 mM HEPES, pH 7.2). As observed for the phosphorylated peptide, chemosensor **2** enhanced its fluorescence intensity upon binding to the phosphoprotein. The emission of **2** considerably increased in the presence of 0.15 equiv of the phospho-α-casein, whereas the emission slightly increased by addition of dephospho-α-casein. In addition to the emission enhancement, its emission maximum shifts from 438 to 470 nm in the case of phospho-α-casein. This may be due to the excimer formation of **2** upon binding

to the phospho-α-casein because it possesses the adjacently aligned phosphoserine residues, i.e., a hyper-phosphorylated site (α_{S1}-casein, pSer^{66}-pSer^{67}-pSer^{68}) on its surface.[32] Figure 14b shows the titration curves of the integrated fluorescence intensity from 400 to 600 nm. Apparently, phospho-α-casein induced larger fluorescence enhancement of **2** compared to dephospho-α-casein. These fluorescence data in aqueous solution are reasonably consistent with the SDS-PAGE results as shown in Fig. 13, in which a brighter emission is detected at the band of phospho-α-casein compared to that of dephosphorylated one. This system enables the convenient detection of phosphate groups attached to tyrosine, serine, or threonine residues of protein at one time, which is difficult in the case of standard Western blotting procedure using phosphoprotein specific antibody. We anticipate that a chemosensor having a brighter fluorophore than anthracene would realize highly sensitive detection of phosphoprotein in SDS-PAGE.[33]

Artificial Chemosensor for Two Phosphate Group on Protein Surface[34]

Recent advances in understanding of post-translational modification revealed that multisite phosphorylation (i.e., hyperphosphorylation) is a common mechanism for regulating protein function in cell signaling pathway.[35] For example, PDGFR-β (platelet-derived grows factor receptor-β), a membrane-bound cytokine receptor, exposes multiple tyrosine residues in the cytoplasmic domain. The binding of PDGF to the extracellular domain induces auto-phosphorylation at these tyrosine residues, which recruits specific signaling proteins containing SH-2 domain, consequently triggering multiple signaling pathways.[36] It is also known that the activity and the cell localization of some transcription factors including p53 and NFAT (nuclear factor of activated T-cells) are regulated by the corresponding hyperphosphorylation process.[6] It addition, much attention has been focused on the abnormal hyperphosphorylation of tau protein.[37] This is because tau is multiphosphorylated to a higher extent to the normal tau (~10 Ser/Thr residues within the repeat domain) and aggregates into tau filaments, which are a hallmark of several neurodegenerative disorders including Alzheimer's disease.

As another approach to recognize phosphorylated protein surface by synthetic small molecules, we designed some chemosensors that are able to interact with a multisite phosphorylation domain of a protein. They possess bipyridine as a spacer unit and two Zn(II)–dpa sites as phosphate binding sites, which are juxtaposed at an appropriately distal position; they are thereby expected to enable the cross-linking interaction with two phosphate groups on a protein surface (Fig. 1). We initially attempted the CD screening study in order to evaluate the binding ability of the chemosensors with a series of the bis-phosphorylated model peptides, in which the α-helix content of the peptide was measured upon addition of the chemosensors. The binuclear chemosensors **6** and **7** considerably induced α-helix formation of the peptides having two phosphoserine (p-Ser) residues (pS-5,16, -9,16, and -12,16 peptides), whereas they did not affect the secondary structure of the mono-phosphorylated peptide (pS-16) (Fig. 15). The most significant CD increase (up to 30% induction of helical conformation) was observed in the combination of **7** with pS-9,16 peptide. On the other hand, mononuclear chemosensors **9** and **10** less effectively induced the helical conformation of the peptides (Fig. 16). The binding affinity of pS-9,16 peptide with **7** was evaluate by the CD titration to give the affinity constant as 1.6×10^6 (K_{app}, M^{-1}), the value of which is over 100-fold stronger than that of the interaction between mono-nuclear complex **5** with phenyl phosphate ($K_{app} = 3\sim4 \times 10^3\ M^{-1}$) as described above. These results strongly suggest that the two-point interaction between the Zn(II)–dpa sites of the chemosensor and the two p-Ser residues of the peptide occurs to induce α-helical structure via cross-linking stabilization. The chemosensor **7** acts not only as a peptide binder, but also as a fluorescence chemosensor toward the bis-phosphorylated peptide. The emission intensity of **7** at 389 nm gradually decreases upon addition of pS-9,16 peptide, and the saturation

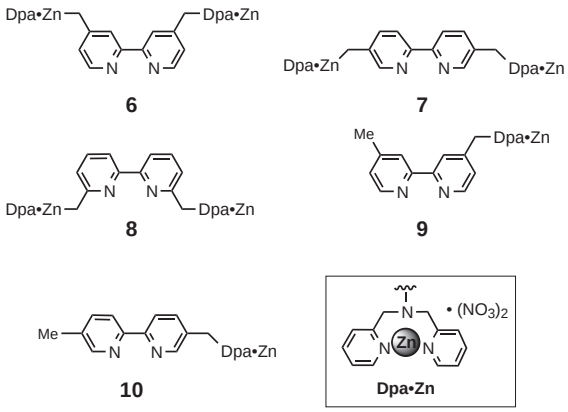

pS-5,16: Ac-**AEAApSKEAAAKEAAApSA**-NH_2

pS-9,16: Ac-**AEAAAKEApSAKEAAApSA**-NH_2

pS-12,16: Ac-**AEAAAKEAAAKpSAAApSA**-NH_2

pS-16: Ac-**AEAAAKEAAAK EAAApSA**-NH_2

CTD-2P: H-**TSPSYpSPTpSPS**-NH_2

CTD-1P: H-**TSPSYSPTpSPS**-NH_2

Fig. 15. Structure of bipyridyl-type chemosensors and sequence of phosphopeptides.

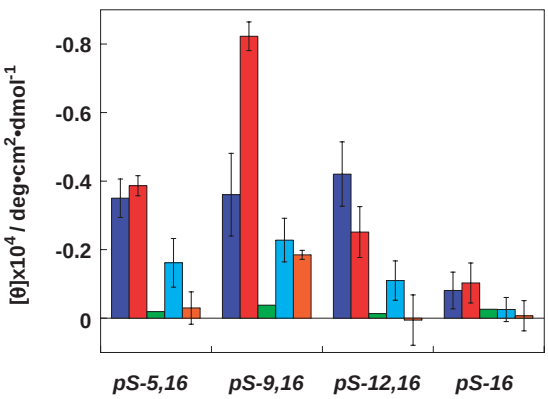

Fig. 16. θ value change (at 222 nm) of phosphopeptides (20 μM) upon addition of bipyridyl-type chemosensor **6** (■), **7** (■), **8** (■), **9** (■), and **10** (■). Measurement conditions: 10 mM borate buffer, pH 8.0, and 10 °C.

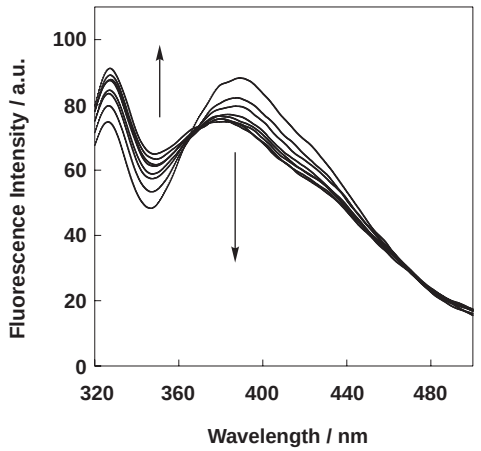

Fig. 17. Fluorescence spectral change of **7** (5 μM) upon addition of pS-9,16 peptide. Measurement conditions: 10 mM borate buffer, pH 8.0, and 20 °C.

Table 4. Apparent Binding Constants ($K_{app} \times 10^{-6}$, M^{-1}) of **7** with the Various Peptides Determined by the Peptide-Induced Fluorescence Change[a)]

pS-5,16	pS-9,16	pS-12,16	pS-16
0.75 ± 0.09	2.0 ± 0.46	0.72 ± 0.10	0.05 ± 0.02

a) The errors were calculated using the data of three titration experiments. Measurement conditions: 10 mM borate buffer, pH 8.0, and 20 °C.

curve of the fluorescent intensity plot afforded the binding constant (K_{app}) of $2.0 \times 10^6\,M^{-1}$ (Fig. 17), the value of which is almost identical with that obtained from CD titration. The binding affinities of **7** for other peptides evaluated by the fluorescence titration are summarized in Table 4. It is noteworthy that the binding of **7** for pS-9,16 ($K_{app} = 2.0 \times 10^6\,M^{-1}$) is over 40-fold larger than that for the mono-phosphorylated pS-16 peptide ($K_{app} = 4.8 \times 10^4\,M^{-1}$), indicating that **7** can discriminate the number of phosphorylation site on the peptide. On the other hand, the binding selectivity seems moderate among the bis-phosphorylated peptides, probably due to the fluctuation of the peptide conformation.

We further evaluated the cross-linking binding property of the chemosensor **6** with the phosphorylated peptides (CTD-1P and -2P), a segment of native protein, by ITC measurement. The CTD peptides possess a sequence of the multiple Tyr-Ser-Pro-Thr-Ser-Pro-Ser heptad repeat found in the CTD (C-terminal domain) of RNA polymerase II.[38] The thermodynamic parameters obtained by ITC experiments are summarized in Table 5. These interactions are again endothermic entropy-driven processes ($\Delta H > 0$), as observed in the interactions between the anthracene-type chemosensor **1** with the phosphopeptides. The chemosensor **6** strongly binds to bis-phosphorylated CTD-2P peptide with a binding affinity (K_{app}) of $2.8 \times 10^6\,M^{-1}$. On the other hand, the binding with mono-phosphorylated CTD-1P peptide ($K_{app} = 1.6 \times 10^4\,M^{-1}$) is considerably weaker than that with CTD-2P peptide, suggesting that the two-point metal–ligand interaction works effectively in aqueous medium. Interestingly, the binding of the substitution isomer **7** with CTD-2P peptide is weaker compared to the corresponding interaction of **6** and not the 1:1 binding stoichiometry. This result may suggest that the distance of the two Zn(II)–dpa sites, which is mainly defined by their substitution position and molecular flexibility, is crucial to form the tight cross-linking complex.

Table 5. Stoichiometry (n), Binding Constant (K_{app}, M^{-1}), Enthalpy (ΔH, kcal mol^{-1}), and Entropy ($T\Delta S$, kcal mol^{-1}) for Interaction of Chemosensor **6** and **7** with the CTD Peptides[a)]

Peptide		**6**	**7**
CTD-2P	n	0.99 ± 0.01	0.70 ± 0.00
	K_{app}	$(2.80 \pm 0.36) \times 10^6$	$(4.83 \pm 0.23) \times 10^5$
	ΔH	4.53 ± 0.04	6.79 ± 0.26
	$T\Delta S$	13.3	14.5
CTD-1P	n	1.22 ± 0.01	1.07 ± 0.07
	K_{app}	$(1.62 \pm 0.03) \times 10^4$	$(7.39 \pm 0.49) \times 10^3$
	ΔH	4.43 ± 0.54	2.54 ± 0.20
	$T\Delta S$	10.2	7.81

a) Measurement conditions: 50 mM HEPES, pH 7.2, and 25 °C.

Conclusion

In this article, we presented the molecular recognition and fluorescence sensing properties of the binuclear Zn(II)–dpa complexes toward phosphorylated protein/peptide. Our study clearly indicated that the cooperative use of the metal–ligand interaction is powerful in recognition of single or two phosphate group(s) on a protein/peptide surface under the neutral aqueous conditions. Indeed, chemosensors **1** and **2** exhibit the strong binding affinities for the highly negatively charged peptide with a binding affinity of nearly $10^7\,M^{-1}$. It was also demonstrated that the cross-linking interaction is effective for the recognition of the bis-phosphorylated peptide with a strong binding affinity. A key issue in these chemosensors is the recognition selectivity. Actually, the binding selectivity among phosphorylated protein/peptide and discrimination against biological diphosphate derivatives (ATP and ADP) are not satisfactory as this stage. Further structural modification should be conducted in order to obtain selective recognition properties. Although it is very tough to overcome this problem, a general solution may be provided by a combinatorial usage of a biological molecule or other artificial system that can recognize the phosphoprotein surface of interest. Introduction of these second recognition sites into the chemosensor may achieve the desired binding selectivity toward a specific phosphoprotein. We also discovered that the unique fluorescence sensing mechanism of **1** and **2** involves the canceling of PET quenching through the phosphate anion induced Zn(II) complexation. This sensing ability has been successfully applied for the real-time monitoring of PTP1B-catalyzed dephosphorylation process. However, the more dynamic fluorescence change including a dual-emission/excitation spectral shift is required for the precise and high-resolution detection of protein phosphorylation/dephosphorylation event under complicated biological conditions. The brighter fluorescence with a longer excitation and emission wavelength is also desirable for various biological applications. We believe that improve-

ment in these points step by step will afford a sophisticated molecular tool that is useful for dissection of complicated phosphorylation-based signaling networks, i.e. phosphoproteome and kinome analysis.[39,40] Our research is now in progress along this line.

References

1 B. M. Sefton, T. Hunter, *Protein Phosphorylation*, Academic Press, New York, **1998**.

2 L. N. Johnson, R. J. Lewis, *Chem. Rev.* **2001**, *101*, 2209.

3 B. L. Canagarajah, A. Khokhlatchev, M. H. Cobb, E. J. Goldsmith, *Cell* **1997**, *90*, 859.

4 M. B. Yaffe, *Nat. Rev.* **2002**, *3*, 177.

5 M. B. Yaffe, A. E. H. Elia, *Curr. Opin. Cell Biol.* **2001**, *13*, 131.

6 C. I. Holmberg, S. E. F. Tran, J. E. Eriksson, L. Sistonen, *Trends Biochem. Sci.* **2002**, *27*, 619.

7 H. Zhang, X. Zha, Y. Tan, P. V. Hornbeck, A. J. Mastrangelo, D. R. Alessi, R. D. Polakiewicz, M. J. Comb, *J. Biol. Chem.* **2002**, *277*, 29279.

8 L. Bonetta, *Nat. Methods* **2005**, *2*, 225.

9 M. Sato, T. Ozawa, K. Inukai, T. Asano, Y. Umezawa, *Nat. Biotechnol.* **2002**, *20*, 287.

10 D. S. Lawrence, *Acc. Chem. Res.* **2003**, *36*, 401.

11 A. Ojida, M. Yoshifumi, T. Kohira, I. Hamachi, *Biopolymers* **2004**, *76*, 177.

12 A. Ojida, Y. Mito-oka, M. Inoue, I. Hamachi, *J. Am. Chem. Soc.* **2002**, *124*, 6256.

13 A. Ojida, Y. Mito-oka, K. Sada, I. Hamachi, *J. Am. Chem. Soc.* **2004**, *126*, 2454.

14 P. D. Beer, P. A. Gale, *Angew. Chem., Int. Ed.* **2001**, *40*, 486.

15 R. Martínez-Máñez, F. Sancenón, *Chem. Rev.* **2003**, *103*, 4419.

16 M. E. Huston, E. U. Akkaya, A. W. Czarnik, *J. Am. Chem. Soc.* **1989**, *111*, 8735.

17 S. Aoki, E. Kimura, *Rev. Mol. Biotechnol.* **2002**, *90*, 129.

18 S. Mizukami, T. Nagano, Y. Urano, A. Odani, K. Kikuchi, *J. Am. Chem. Soc.* **2002**, *124*, 3920.

19 S. L. Tobey, E. V. Anslyn, *J. Am. Chem. Soc.* **2003**, *125*, 14807.

20 D. E. Wilcox, *Chem. Rev.* **1996**, *96*, 2435.

21 F. Diederich, K. Dick, *J. Am. Chem. Soc.* **1984**, *106*, 8024.

22 Z. Songyang, L. C. Cantley, *Trends Biochem. Sci.* **1995**, *20*, 470.

23 L. A. Pinna, M. Ruzzene, *Biochim. Biophys. Acta* **1996**, *1314*, 191.

24 J. Krieg, T. Hunter, *J. Biol. Chem.* **1992**, *267*, 19258.

25 I. Wadsö, *Chem. Soc. Rev.* **1997**, *26*, 79.

26 M. Rekharsky, Y. Inoue, S. Tobey, A. Metzger, E. Anslyn, *J. Am. Chem. Soc.* **2002**, *124*, 14959.

27 B. Valeur, I. Leray, *Coord. Chem. Rev.* **2000**, *205*, 3.

28 C.-A. Chen, R.-H. Yeh, D. S. Lawrence, *J. Am. Chem. Soc.* **2001**, *124*, 3840.

29 M. D. Shults, B. Imperiali, *J. Am. Chem. Soc.* **2003**, *125*, 14248.

30 T. O. Johnson, J. Ermolieff, M. R. Jirousek, *Nat. Rev. Drug Discovery* **2002**, *1*, 696.

31 A. Ojida, T. Kohira, I. Hamachi, *Chem. Lett.* **2004**, *33*, 1024.

32 H. E. Swaissgood, *Developments in Dairy Chemistry-1 Proteins*, Applied Science, London, **1982**.

33 T. H. Steinberg, B. J. Agnew, K. R. Gee, W.-Y. Leung, T. Goodman, B. Schulenberg, J. Hendrickson, J. M. Beechem, R. P. Haugland, W. F. Patton, *Proteomics* **2003**, *3*, 1128.

34 A. Ojida, M. Inoue, Y. Mito-oka, I. Hamachi, *J. Am. Chem. Soc.* **2003**, *125*, 10184.

35 X.-J. Yang, *Oncogene* **2005**, *24*, 1653.

36 C. H. Heldin, B. Westermark, *Physiol. Rev.* **1999**, *79*, 1283.

37 J. Eidenmüller, T. Fath, A. Hellwig, J. Reed, E. Sontag, R. Brandt, *Biochemistry* **2000**, *39*, 13166.

38 Y.-X. Yu, Y. Hirose, X. Z. Zhou, K. P. Lu, J. L. Manley, *Genes Dev.* **2003**, *17*, 2765.

39 D. E. Kalume, H. Molina, A. Pandey, *Curr. Opin. Chem. Biol.* **2003**, *7*, 64.

40 S. A. Johnson, T. Hunter, *Nat. Methods* **2005**, *2*, 17.

Akio Ojida was born in Fukuoka in 1968. He received his Ph.D. (1995) from Kyushu University. He was a postdoctoral researcher at the Institute for Molecular Science (1995–1996), and was a researcher at Medicinal Research Laboratories, Takeda Chemical Industries, Ltd. (1997–2001). In 2001–2003, he was a research associate at the Graduate School of Engineering, Kyushu University. Currently, he is research associate at the Graduate School of Engineering, Kyoto University. His research interests focus on medicinal chemistry and chemical biology, especially on artificial molecular recognition and sensing systems for proteins.

Prof. Itaru Hamachi had obtained his Ph.D. from Kyoto University, Japan, in 1988 and was engaged as an assistant professor in Kyushu University (Emeritus Professor Kunitake's group) at the same time. In 1992, he moved to Prof. Shinkai's group as an associate professor, and then was promoted to a full professor in IFOC, Kyushu University, in 2001. He moved to the Department of Synthetic Chemistry and Biological Chemistry, Kyoto University, in 2005. He is also now a PRESTO investigator (JST). His research interests are in the range of bio-organic and bioinorganic chemistry, protein engineering, chemical biology, and supramolecular chemistry.